Rongqing Chen*, and Knut Moeller

Detection of Outdated Structural Priors in the Discrete Cosine Transformation-based Electrical Impedance Tomography Algorithm

Abstract: Morphological prior information incorporated with the discrete cosine transformation (DCT) based electrical impedance tomography (EIT) algorithm can improve the interpretability of EIT reconstructions in clinical applications. However, an outdated structural prior can yield a misleading reconstruction compromising the accuracy of the clinical diagnosis and the appropriate treatment decision. In this contribution, we propose a redistribution index scaled between 0 and 1 to quantify the possible error in a DCT-based EIT reconstruction influenced by structural prior information. Two simulation models of different tissue atelectasis and collapsed ratios were investigated. Outdated and updated structural prior information were applied to obtain different EIT reconstructions using this simulated data, with which the redistribution index was calculated and compared. When the difference between prior and reality (the redistribution index) became larger and exceeded a threshold, this was considered as an indicator of an outdated prior information. The evaluation result shows the potential of the redistribution index to detect outdated prior information in a DCT-based EIT algorithm.

Keywords: electrical impedance tomography, simulation, prior information, redistribution index.

https://doi.org/10.1515/cdbme-2021-2172

1 Introduction

Electrical Impedance Tomography (EIT) is applied to the visualization of the regional lung ventilation and aeration distribution. EIT uses the current induced voltage changes through the electrodes attached on the surface of the chest for image reconstruction[1]. This technique has proven useful to reduce the risk of ventilator induced lung injury (VILI) on mechanically ventilated patients in the intensive care unit (ICU)[2]. However, low spatial resolution, blurred anatomical alignment, and reconstruction induced artefacts hinder the interpretation of the status of patients in clinical settings. Introducing structural prior information into EIT images will be helpful for clinicians in forming a more direct comprehensive insight[3].

Prior information can vary but is usually based on tissue conductivities or anatomical constraints or both. Assigning mentioned properties to a predefined area might be the most common approach to embed prior information in the EIT reconstruction algorithm. e.g., Glidewell et al. use the shape of the lungs to group FEM elements and to assign different impedance values[4]. Another principle to include prior information is introduced as a subset of constraint basic functions. Vauhkonen et al. chose a series of representative ensembles of expectable conductivity distributions based on physiological information within the body[5].

Generally, these former attempts generated a universal prior for all patients. To allow a more patient-specific prior, Schullcke et al. proposed a novel EIT algorithm with the prior as a subset of basic functions using patient related morphological images taken, e.g., from CT or MRI images[6]. The generation of the constraining subsets are obtained from the discrete cosine transformation (DCT) of the related morphological images.

Even though this algorithm has shown attractive results, it comes with the same problem as all priors always do: results are just as good as the validity of the prior assumptions. The DCT-based prior might lose validity during hospitalization and treatment since the status of the patient is changing over time. The outdated prior information might induce a risk in terms of misleading interpretation of the results.

The objective of this work is to introduce an effective approach to detect outdated prior information applied to the DCT-based EIT algorithm. A redistribution index is proposed to quantify the difference between the constrained and the

***Corresponding author: Rongqing Chen:** Institute of Technical Medicine, Furtwangen University, Jakob-Kienzle-Str. 17, Villingen Schwenningen, Germany, e-mail: chr@hs-furtwangen.de
Knut Moeller: Institute of Technical Medicine, Furtwangen University, Jakob-Kienzle-Str. 17, Villingen Schwenningen, Germany

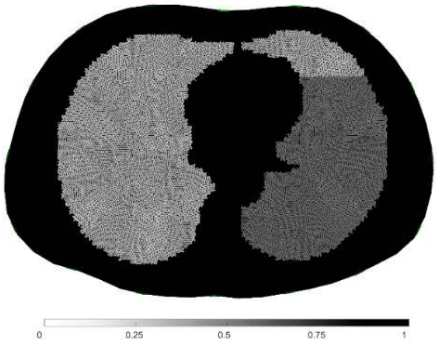

Figure 1: The FEM models used for simulation: collapse model (75% of the left lobe).

unconstrained DCT results. Simulations experiments with different scales of tissue atelectasis and collapse were conducted for evaluation purpose. Redistribution indexes were calculated using the constrained and the unconstrained DCT results of every simulated scale. At last, a threshold value of the redistribution index was determined to identify outdated prior information.

2 Method

2.1 DCT-based EIT reconstruction

The reconstruction of conductivity distribution $\hat{x}$ in difference EIT is presented in eq. 1, where vector $\boldsymbol{x} = \boldsymbol{\sigma} - \boldsymbol{\sigma}^{baseline}$ is the change in internal conductivity distribution $\boldsymbol{\sigma}$ and $\boldsymbol{y} = \boldsymbol{v} - \boldsymbol{v}^{baseline}$ is a vector containing the differences of measured voltage v.

$$\hat{\boldsymbol{x}} = argmin_x\{\| \boldsymbol{F}(x) - \boldsymbol{y} \|_2^2 + \lambda^2 \| \boldsymbol{R}\boldsymbol{x} \|_j^j\} \quad (1)$$

if only small conductivity changes are observed, the forward model $\boldsymbol{F}(x)$ can be linearized around a reference conductivity $\boldsymbol{\sigma}^{baseline}$ such that $\boldsymbol{F}(x) \approx \boldsymbol{J}\boldsymbol{x}$, where $J_{i,j} = \frac{\partial y_i}{\partial x_j}\Big|_{\sigma_{ref}}$ forms a Jacobian matrix $\boldsymbol{J}$. An element $J_{i,j}$ maps small voltage changes at the position i of y to a conductivity change of the element j within the discretized domain in a FEM model. The $\boldsymbol{R}$ is a regularization term which can be chosen from several options. Equation 1 can be solved in a closed form with linearization:

$$\hat{\boldsymbol{x}} = (\boldsymbol{J}^T\boldsymbol{J} + \lambda^2\boldsymbol{R})^{-1}\boldsymbol{J}^T\boldsymbol{y} = \boldsymbol{B}\boldsymbol{y} \quad (2)$$

where the matrix B is the reconstruction matrix which calculates the impedance distribution variation from the measured boundary voltages. One common method to include prior information is to group different tissue properties in the setting of $\boldsymbol{\sigma}^{baseline}$ on which $\boldsymbol{J}$ is depending[5].

The other method to include constraining prior information is to introduce basic functions $s_1(p,q), s_2(p,q), \dots, s_M(p,q)$ to modify the Jacobian matrix $\boldsymbol{J}$. The reconstructed conductivity change $\hat{\boldsymbol{x}}$ in eq. 2 is written:

$$\hat{\boldsymbol{x}} = (\boldsymbol{J}\boldsymbol{S}^T\boldsymbol{J}\boldsymbol{S} + \lambda^2\boldsymbol{R})^{-1}\boldsymbol{J}\boldsymbol{S}^T\boldsymbol{y} = \boldsymbol{B}\boldsymbol{y} \quad (3)$$

where $\boldsymbol{S} \in R^{N\times M}$ represents the matrix of constraining basic functions, N is the number of the elements in the FEM.

In this contribution, the basic function subset $\boldsymbol{S}$ is obtained by element-wise mapping of FEM-elements to basis vectors of a Discrete Cosine Transform (DCT) of the patient specific morphological image A.

$$V_{p,q} = \sum_{m=0}^{M-1}\sum_{n=0}^{N-1} A_{m,n} \cdot D(p,q)_{m,n} \quad (4)$$

where the cosine function combinations implemented in the basic function subset are formed as $\mathrm{D(p,q)_{m,n}} = \alpha_p\alpha_q \cos\frac{(2m+1)p\pi}{2M} \cdot \cos\frac{(2n+1)q\pi}{2N}$. p and q are the frequencies of the cosine function at the x-axis and y-axis, respectively. In this contribution p and q are chosen as 15 frequencies at either axis as $p, q \in (0,1,\dots,14)$. The different choices of the image A will yield different levels of constraints in the prior, e.g. Hounsfield unit in a CT image will constrain the reconstruction at different parts within the lung area, resulting in a clear anatomical structure; but a binary lung contour does not limit the reconstruction within the lung area.

The multiplication of $D(p,q)_{m,n}$ and an anatomical binary lung image $P_{m,n}$ yields matrix $C(p,q)_{m,n} = P_{m,n} \cdot D(p,q)_{m,n}$. The columns of the basic function subset is determined as $s_i = T\big(C(p,q)\big)$, where T is a mapping function assigning each pixel of $C(p,q)$ to the FEM elements which covers the corresponding pixel[6],[7].

2.2 Simulation

The simulations were carried out with MATLAB R2019a (Mathworks, Natick, MA, USA) and with the EIDORS toolbox[8]. In the simulation, initially the FEM-elements belonging to lung area were assigned to a conductivity of $\boldsymbol{\sigma}_{lung}^{initial} = 0.5$, the remaining elements were set to $\boldsymbol{\sigma}_{non-lung}^{initial} = 1$. With this initial configuration, $v_{initial}$ was generated.

The first simulation involved different scales of dorsal lung area atelectasis from 0% to 50%. Ventilated lung tissue was set to a conductivity of $\boldsymbol{\sigma}_{lung}^{ventilated} = 0.25$, while the collapsed area remained at $\boldsymbol{\sigma}_{lung}^{atelectasis} = 0.5$. This configuration yielded the $\boldsymbol{v}_{atelectasis}$ for reconstruction. The second simulation used the same values for conductivity configuration but involved different scales of only left lung collapse from 0% to 100%. This simulation yielded the $\boldsymbol{v}_{collapse}$. One example of a simulation setting is depicted in Fig. 1.

In the reconstruction part, 25% of Gaussian noise was superimposed on to the $\boldsymbol{v}_{atelectasis}$ and $\boldsymbol{v}_{collapse}$. To prevent the 'inverse-crime', different meshes were used for simulating the voltage changes and image reconstruction. During reconstruction, three different kinds of prior information, namely lung contour (non-constrained prior), accurate prior, 100% left lung collapse prior or 50% dorsal atelectasis prior (fixed constrained prior), were adopted into the DCT approach. These two simulation experiments were used to evaluate a criterion to detect an outdated fixed constrained prior.

2.3 Redistribution index

A DCT-based basic function subset generated from a morphological image can impose more constraints into reconstruction in addition to the lung shape. It can be determined by from the corresponding Hounsfield scale units in the CT image which derives and is coded into the $T\big(C^c(p,q)\big)$. If only a lung shape without details is specified, the $T\big(C^{nc}(p,q)\big)$ will allow the reconstruction in the whole lung area. The redistribution index is proposed to quantify the amount of the 'leaking' reconstruction from a constrained area to a non-constrained area using the same measurement data, or more theoretically, the redistribution of the pixel value histogram. The redistribution index is defined by eq. 5:

$$RI = \frac{\sum_{xy\in \text{cons}}\{(\hat{\boldsymbol{x}}^{nc}_{xy} - \hat{\boldsymbol{x}}^{c}_{xy}\})}{\sum_{xy\in\hat{\boldsymbol{x}}^{c}_{xy}} \hat{\boldsymbol{x}}^{c}_{xy}} \qquad (5)$$

$xy \in$ cons expresses the constrained area in the morphological constrained area, $\hat{\boldsymbol{x}}^{c}$ is the DCT approach result using the constrained area prior, and $\hat{\boldsymbol{x}}^{nc}$ is the DCT approach result without the constrained area prior. Equation 5 will yield a value between 0 and 1. The flowchart to calculate the redistribution index is depicted in Fig. 2.

3 Results

Simulation reconstruction examples, namely 50% left lung collapse and 25% dorsal atelectasis, are shown in Fig. 3a. The redistribution index was calculated and depicted in Fig. 3b. The DCT approach results, which used the prior of 100% collapse or 50% atelectasis, only allowed the reconstruction within the pre-defined area. Thus, these results cannot imply the real simulation status. From the depicted redistribution indexes of either simulation, redistribution index increased as the atelectasis scale or collapse scale decreased. In other words, when the difference between the real status and the fixed constrained prior information became more notable, an

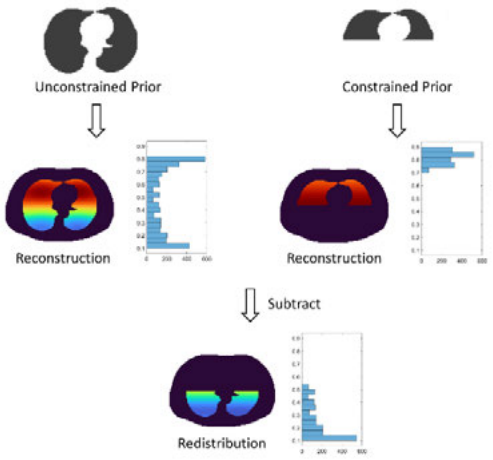

Figure 2: The redistribution index calculation flowchart. The examples were derived from a simulation of 25% atelectasis. The example constrained prior is set as 50% atelectasis.

increase will be expected in the redistribution index. When this difference becomes unbearable, the redistribution index will reach to a threshold. Currently, for the clinical EIT evaluation there exists no consensus on the best criterion to identify an EIT result that is misleading. We note that the control of the prior-reality difference within 30% will yield a rather tolerate result. Thus, at this difference point the redistribution index is around 0.4, which was used as a preliminary threshold. While for the reconstructions from the accurate prior, the redistribution indexes are smaller and remain below the threshhold, e.g., for the 31% atelectasis scale simulation, the redistribution index for fixed prior exceeds 0.4, but for the accurate prior the index is 0.09, which is almost 80% lower.

4 Discussion

In this contribution, we proposed the redistribution index with the aim to detect an outdated morphological prior information used in the novel DCT-based EIT algorithm. A redistribution index threshold was based on two simulation experiments in terms of collapse and atelectasis scales, respectively. It was demonstrated that there is a straightforward way to quantify the effect of an outdated constrained prior on the result of the DCT approach. In Fig. 3b, an increasing trend of redistribution index was obvious when the difference between the fixed constrained prior and real status became more notable. When the redistribution index reached 0.4, we can assume that the pre-defined constrained prior outdated. It is recommended that the integrated priors in the DCT-based EIT algorithm should be checked and updated at this point, e.g., by available patient measurements or by predicting potential changes based on pathophysiology or both.

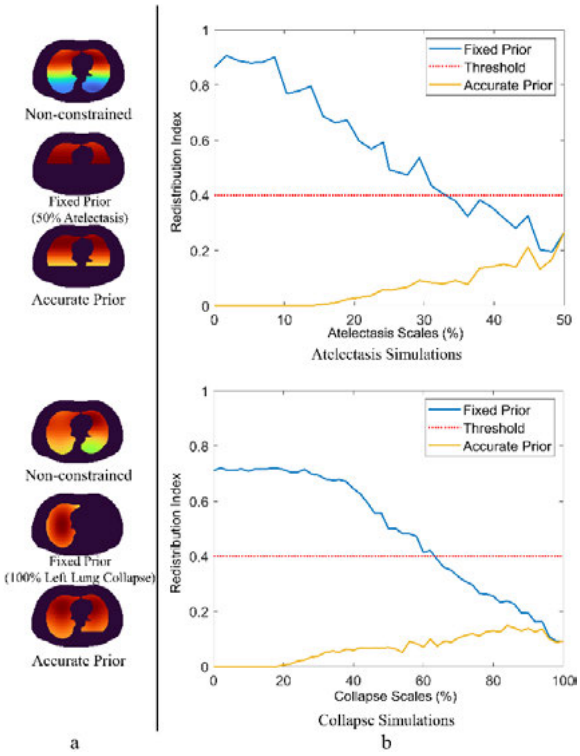

Figure 3: Exemplary DCT approach results and corresponding redistribution index from the two simulation experiments. (a) DCT results with different priors employed. Upper: Examples from the simulation of 25% of atelectasis; Lower: Examples from 25% of the left lung collapse. (b) Redistribution indexes calculated from the two-scope simulations.

It is worth noting that the accurate prior employed results are expected to be accurate in the simulation, but a redistribution was still observed. This can be explained by the construction of the constraint DCT reconstruction. The non-constrained prior DCT approach allows the reconstruction in the entire lung area, and the spatial resolution of EIT is low, i.e., shows a smoothing effect. Even though, the redistribution indexes for the accurate prior results remained much lower than the threshold.

One of the limitations of this research is that the threshold is derived from just two simulation experiments. It should be evaluated by further research. In simulations, the conductivity distributions were based only on a simple physiological assumption. While in clinical settings, the patients are expected to suffer from several symptoms. It should be more accurate to yield a threshold from clinical data.

Nevertheless, the redistribution index can suggest the potential changing of the patient status. Thus, it could be used as an indicator for an outdated prior in the DCT-based EIT approach. Updating the prior information in the DCT approach can facilitate the accurate interpretation of EIT results.

5 Conclusion

The redistribution index was proposed, and a preliminary evaluation was done with the help of simulations. The evaluation result reveals the potential of the redistribution index to detect an outdated prior in the DCT-based EIT algorithm. Considering the calculation method of the redistribution index, it should be possible to extend this definition to other EIT algorithms using prior information.

Author Statement

Research funding: This research was partially supported by the German Federal Ministry of Education and Research (MOVE, Grant 13FH628IX6) and H2020 MCSA Rise (#872488 DCPM). Conflict of interest: Authors state no conflict of interest. Informed consent: Informed consent has been obtained from all individuals included in this study. Ethical approval: The research related to human use complies with all the relevant national regulations, institutional policies and was performed in accordance with the tenets of the Helsinki Declaration, and has been approved by the authors' institutional review board or equivalent committee.

References

[1] I. Frerichs, P. A. Dargaville, T. Dudykevych, and P. C. Rimensberger, "Electrical impedance tomography: A method for monitoring regional lung aeration and tidal volume distribution?" Intensive Care Medicine, vol. 29, no. 12, pp. 2312–2316, 2003-12-01, 2003-12-1.

[2] Z. Zhao, D. Steinmann, I. Frerichs, J. Guttmann, and K. Moller, "PEEP titration guided by ventilation homogeneity: A feasibility study using electrical impedance tomography," Critical Care, vol. 14, no. 1, p. R8, 2010.

[3] S. Milne and G. G. King, "Advanced imaging in COPD: Insights into pulmonary pathophysiology," Journal of thoracic disease, vol. 6, no. 11, p. 1570, 2014.

[4] M. Glidewell and K. T. Ng, "Anatomically constrained electrical impedance tomography for anisotropic bodies via a two-step approach," IEEE Transactions on Medical Imaging, vol. 14, no. 3, pp. 498–503, 1995-09, 1995-9.

[5] M. Vauhkonen, J. Kaipio, E. Somersalo, and P. Karjalainen, "Electrical impedance tomography with basis constraints," Inverse problems, vol. 13, no. 2, p. 523, 1997.

[6] B. Schullcke, B. Gong, S. Krueger-Ziolek, M. Soleimani, U. Mueller-Lisse, and K. Moeller, "Structural-functional lung imaging using a combined CT-EIT and a discrete cosine transformation reconstruction method," Scientific reports, vol. 6, p. 25951, 2016.

[7] R. Chen and K. Möller, "Global Inhomogeneity Index Evaluation of a DCT-based EIT Lung Imaging," Curr. Dir. Biomed. Eng., vol. 6, no. 3, pp. 36–39, Sep. 2020, doi: 10.1515/cdbme-2020-3010.

[8] A. Adler and W. R. B. Lionheart, "Uses and abuses of EIDORS: An extensible software base for EIT," Physiological Measurement, vol. 27, no. 5, pp. S25–S42, 2006-04, 2006.